Review

Simulation of the Process of Injection of Liquid Sulfur Dioxide into a Porous Reservoir Initially Saturated with Methane and Ice

Ilias K. Gimaltdinov * and Maksim V. Stolpovskii

Department of Physics, Ufa State Petroleum Technological University, 1 Kosmonavtov Str., 452064 Ufa, Russia; s_maxim.pmm@mail.ru

* Correspondence: iljas_g@mail.ru; Tel.: +7-3472- 242-07-18

Abstract: The paper presents the results of modeling the problem of injecting liquid sulfur dioxide into a porous reservoir initially saturated with methane and ice. The model presented in the paper assumes the formation of three different regions, namely, the near one, saturated with liquid SO_2 and its hydrate; the far one, containing methane and ice, and the intermediate one, saturated with methane and water. The effects of various parameters of the porous medium and injected SO_2 on the nature of the course of the hydrate formation process have been studied. It is shown that with a decrease in reservoir permeability or injection pressure, the length of the intermediate region decreases, which in the limiting case means the formation of SO_2 hydrate in the mode without the formation of an extended region saturated with methane and water. It is shown that such a regime is also typical for the case of high initial injection pressures, as well as low values of the initial reservoir temperature and injection temperature.

Keywords: mathematical modeling; non-isothermal flow; porous medium; gas hydrates

MSC: 76-10; 35Q79

1. Introduction

Gas hydrates or clathrates are crystalline compounds formed under certain thermobaric conditions and containing gas and water in their composition. Under certain thermobaric conditions, gas hydrates are formed mainly from gas and water (or ice) [1,2]. Since the sixties of the twentieth century the emphasis in the study of gas hydrates began to shift towards the extraction of gas from their composition. At that time, the Messoyakh gas hydrate field, deposits in the Mackenzie Delta, and natural accumulations of hydrates at the bottom of the seas and oceans were discovered. At present, the volume of gas in the composition of gas hydrates is estimated at about 10^{16} m^3 [3]. Therefore, the development of gas from such fields is quite relevant. In particular, the following methods of gas production from the gas hydrate composition have been proposed [4,5]: thermal, depressurization, and injection of inhibitors. These methods of extracting gas from the composition of the gas hydrate are called traditional methods. It should be noted that the methods of gas production from the gas hydrate composition described above are, for the most part, inefficient and costly.

A fairly large number of theoretical and experimental works have been devoted to the problems of gas production from the composition of gas hydrates. Among the theoretical works published over the past 15 years, the following can be distinguished [6–12]. It should be noted that these works are devoted to the theoretical study of traditional methods for the development of gas hydrate deposits. At the same time, the mathematical models are based on the methods and equations of the mechanics of multiphase media (the system of basic equations necessarily includes the continuity equation, Darcy's law, the continuity equation, and the energy equation). The most complete mathematical models of the formation and decomposition of gas hydrates, which are close to real conditions for the

 doi:10.20944/preprints202306.1087.v1

development of gas hydrate deposits, are presented in [13–17]. Modeling of gorenje hydrate methane with account of the non-stationary process of its dissociation in the powder layer is presented, in particular, in [18].

In contrast to theoretical works, experimental works on the study of methane extraction from methane gas hydrate also include works on the method of replacing methane with carbon dioxide in methane gas hydrate. In particular, in [19,20], the very possibility of the reaction of substitution of methane molecules by carbon dioxide molecules in methane gas hydrate was convincingly proved. Also, as a result of the experiments, the following features were established that occur when methane hydrate samples are exposed to carbon dioxide. Thus, if the temperature of the system is below the equilibrium temperature (at a given pressure) of the decomposition of methane gas hydrate into methane and water, then the reaction of replacing methane with carbon dioxide does not release free water [21,22]. In this case, instead of methane hydrate, carbon dioxide hydrate is formed without the formation of an intermediate liquid phase. At the same time, it was shown in [19] that the reaction of replacing methane with carbon dioxide, i.e., occurs with the release of heat. In general, characterizing the experimental work on this topic, it should be noted that in most experimental work, this process is studied in free volume, and not in the pore space. In addition, in experimental studies, studies were carried out, as a rule, in samples of small size and under conditions of thermal and pressure control. Therefore, in these studies, due to the small size of the samples and the maintenance of constant thermobaric conditions, the replacement process is limited primarily by the kinetics of the process. These studies do not provide a complete picture of the processes for the tasks set in the project, since in the case of extended natural reservoirs with constant injection of carbon dioxide into the reservoir, due to the release of latent heat of phase transitions, absorption / release of gas and active mass transfer in a porous medium, the process of replacing methane with carbon dioxide in a gas hydrate will be determined not only by the kinetics of the process, but also by heat and mass transfer in the porous medium itself.

Numerical modeling of the replacement of methane by carbon dioxide in methane gas hydrate is the subject of, in particular, works [23–25]. Basically, they study only the kinetics of the process. At the same time, the formulation of problems in them corresponds to the case when carbon dioxide instantly fills all points of the reservoir saturated with methane and water, i.e. does not take into account the processes of heat and mass transfer in the reservoir itself (at the macrolevel).

It should also be noted that there are a number of theoretical and experimental works on the study of carbon dioxide injection into underground reservoirs in the context of the problem of greenhouse gas utilization. For example, in [26–28], the processes of formation and decomposition of gas hydrates are not studied, but it is proved that the injection of carbon dioxide into underground reservoirs is a fairly effective way of its sequestration. It was also shown in [29,30] that one of the promising methods for utilizing sulfur dioxide is its injection in the liquid phase into depleted natural gas fields. This technique, firstly, provides a fairly reliable conservation of SO_2 in the solid phase at relatively low economic costs, and secondly, it ensures the release of natural gas (methane) from such reservoirs. These solutions for the utilization of industrial gases will help solve a number of environmental problems. Therefore, in the presented work, some features of the injection of liquid sulfur dioxide for porous reservoirs of finite length, initially saturated with methane and ice, are numerically investigated.

The phase diagram (Figure 1) shows the thermobaric conditions for the existence of sulfur dioxide gas hydrate [31]. In the above diagram, curve 1 corresponds to a three-phase equilibrium between gaseous sulfur dioxide, its gas hydrate, and water (ice), curve 2, to a two-phase equilibrium between gaseous and liquid sulfur dioxide, and curve 3, to an equilibrium between liquid sulfur dioxide, its gas hydrate, and water. SO_2 gas hydrate exists above curve 1 and to the left of curve 3, i.e. at sufficiently high pressures and low temperatures. At the upper quadrupole point Q_2 (T_Q = 285.1 K and p_Q = 0.233 MPa), gaseous and liquid sulfur dioxide, as well as its gas hydrate and water, are in equilibrium.

Preprints (www.preprints.org) | NOT PEER-REVIEWED | Posted: 15 June 2023 doi:10.20944/preprints202306.1087.v1

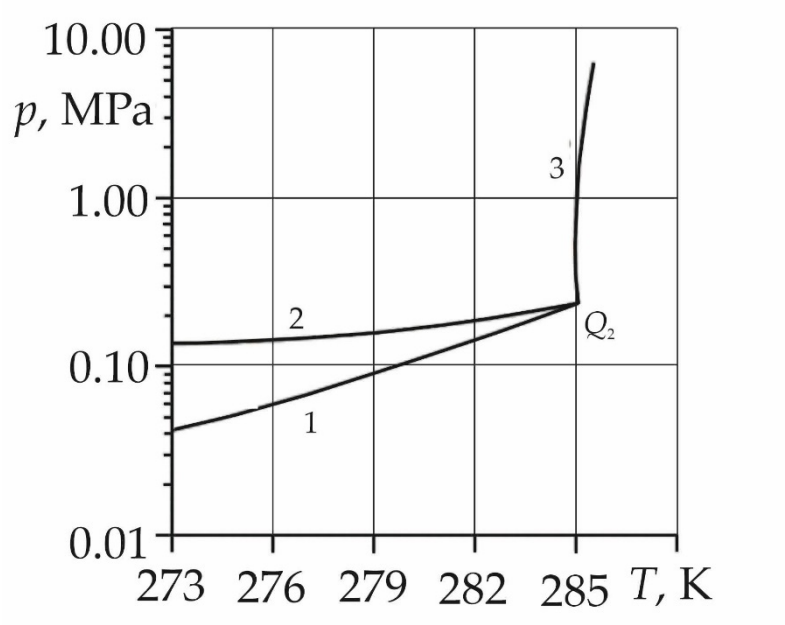

Figure 1. Phase diagram of the SO_2-H_2O system.

Let a porous horizontal layer of length L in the initial state be saturated with ice with initial saturation S_{w0} and methane. We will assume that the initial values of temperature T_0 and pressure p_0 of the formation correspond to the thermodynamic conditions for the existence of sulfur dioxide (in the liquid state) and its gas hydrate (i.e., above curve 2 in Figure 1). Let liquid sulfur dioxide be injected through the left boundary of the formation (x = 0), the pressure p_e and temperature T_e of which correspond to the conditions for the existence of sulfur dioxide gas hydrate. We will assume that in this case three regions are formed in the reservoir: near, far and intermediate. In the near zone, liquid sulfur dioxide and its gas hydrate will be present in the formation pores. The intermediate zone will be saturated with water and methane, while the far zone will be saturated with ice and methane. In this case, two boundaries of phase transitions will appear in the reservoir, separating these areas and moving deep into the reservoir. So, at the near boundary of the phase transition $x = x_{(n)}$, SO_2 gas hydrate is formed from water and sulfur dioxide, and at the far surface of the phase transition $x = x_{(d)}$ ice melting.

2. Basic equations

To describe the processes of heat and mass transfer, accompanied by the formation of sulfur dioxide hydrate and melting of ice, we will use a single-temperature model of the system under consideration with a constant value of porosity. In this case, the skeleton of a porous medium, gas hydrate, water are incompressible and motionless; methane will be considered a calorically perfect gas, and liquid sulfur dioxide will be considered an elastic liquid. In addition, SO_2 hydrate is a two-component system with a mass fraction of the hydrate-forming gas equal to G. The system of basic equations, which is the laws of conservation of mass and energy, Darcy's law and the equation of state under the above assumptions in each of the regions, has the form [32,33]:

$$\begin{gathered}\frac{\partial}{\partial t}\left(\rho_{(i)}\phi S_{(i)}\right)+\frac{\partial}{\partial x}\left(\rho_{(i)}\phi S_{(i)}v_{(i)}\right)=0,\\ \frac{\partial}{\partial t}\left(\rho C T_{(i)}\right)+\rho_{(i)}C_{(i)}\phi S_{(i)}v_{(i)}\frac{\partial T_{(i)}}{\partial x}=\frac{\partial}{\partial x}\left(\lambda\frac{\partial T_{(i)}}{\partial x}\right),\\ \phi S_{(i)}v_{(i)}=-\frac{k_{(i)}}{\mu_{(i)}}\frac{\partial p_{(i)}}{\partial x},\end{gathered} \tag{1}$$

Preprints (www.preprints.org) | NOT PEER-REVIEWED | Posted: 15 June 2023 doi:10.20944/preprints202306.1087.v1

$$\rho_s = \rho_{0s} \cdot \exp\left(\beta(p - p_0)\right), \quad \rho_g = p/R_g T .$$

Here, the subscripts $i = s, m$ refer to the parameters of liquid sulfur dioxide and methane, respectively; ϕ is porosity; $\rho_{(i)}$, $v_{(i)}$, $k_{(i)}$, $C_{(i)}$ and $\mu_{(i)}$ are, respectively, the true density, velocity, permeability, specific heat and dynamic viscosity of the i - phase; p is pressure; T is temperature; $S_{(i)}$ – saturation of pores with the i phase; R_g is the gas constant of methane, β is the volumetric compression ratio of liquid SO_2; ρ_{0s} is the true density of liquid sulfur dioxide corresponding to pressure p_0; ρC and λ are the specific volumetric heat capacity and the thermal conductivity of the system. Since the main contribution to the values of ρC and λ is made by the corresponding parameters of the skeleton of the porous medium, we will assume them to be constant values.

The dependence of the phase permeability coefficient k(i) on saturation S(i) is set based on the Kozeny formula [34]:

$$k_{(i)} = k_0 S_{(i)}^3 \quad (i = 1, 2, 3),$$

where k_0 is the absolute permeability of the reservoir. The subscripts 1, 2 and 3 refer to the parameters of the near, intermediate and far regions.

The conditions for the balance of mass and heat at the near boundary of the phase transition $x = x_{(n)}$, which separates the near and intermediate regions and at which SO_2 hydrate is formed from water and sulfur dioxide, can be represented as:

$$\begin{gathered} -\frac{k_s}{\mu_s}\frac{\partial p_{(1)}}{\partial x} = \phi\left(S_s + \frac{\rho_h G}{\rho_s} S_h\right)\dot{x}_{(n)}, \quad -\frac{k_m}{\mu_m}\frac{\partial p_{(2)}}{\partial x} = \phi S_{(2)}\dot{x}_{(n)}, \\ \phi S_h \rho_h (1-G)\dot{x}_{(n)} = \phi S_l \rho_l \dot{x}_{(n)}, \quad \lambda\frac{\partial T_{(1)}}{\partial x} - \lambda\frac{\partial T_{(2)}}{\partial x} = \phi\rho_h L_h S_h \dot{x}_{(n)} . \end{gathered} \tag{2}$$

Here ρ_h and ρ_l are the densities of hydrate and water, respectively; S_h and S_l are hydrate saturation and water saturation; L_h is the specific heat of SO_2 hydrate formation; $\dot{x}_{(n)}$ is the velocity of the phase transition boundary.

Similarly, the conditions at the far boundary of the phase transition $x = x_{(d)}$, where ice melts, can be represented as:

$$\begin{gathered} -\frac{k_{(2)}}{\mu_m}\frac{\partial p_{(2)}}{\partial x} = -\frac{k_{(3)}}{\mu_m}\frac{\partial p_{(3)}}{\partial x}, \quad \phi S_l \rho_l \dot{x}_{(d)} = \phi S_{w0}\rho_{w0}\dot{x}_{(d)}, \\ \lambda\frac{\partial T_{(3)}}{\partial x} - \lambda\frac{\partial T_{(2)}}{\partial x} = \phi\rho_{w0} S_{w0} L_w \dot{x}_{(d)} . \end{gathered} \tag{3}$$

Here ρ_{w0} and L_w are the density and specific heat of ice melting, respectively; $\dot{x}_{(d)}$ is the velocity of the boundary of the far boundary of the phase transition.

The pressure and temperatures at the boundaries of phase transitions will be considered continuous quantities. In addition, since ice melts at the far boundary of phase transitions $x = x_{(d)}$, we assume that its temperature is $T_{(d)} = 273$ K.

Since the initial ice saturation was assumed to be equal to S_{w0}, then from the equations of systems (2) and (3) for the values of S_l and S_h, one can obtain:

$$S_l = \frac{\rho_{w0} S_{w0}}{\rho_l}, \quad S_h = \frac{\rho_l S_l}{\rho_h (1-G)} = \frac{\rho_{w0} S_{w0}}{\rho_h (1-G)} .$$

The initial conditions, as well as the conditions at the outer boundaries of the reservoir, can be represented as:

$$\begin{gathered} t = 0: \; p = p_0, \; T = T_0 \; (0 \le x \le L); \\ x = 0: \; p = p_e, \; T = T_e \; (t > 0); \end{gathered} \tag{4}$$

Preprints (www.preprints.org) | NOT PEER-REVIEWED | Posted: 15 June 2023 doi:10.20944/preprints202306.1087.v1

$$x = L: \ \frac{\partial p}{\partial x} = 0, \ \frac{\partial T}{\partial x} = 0 \ \ (t > 0).$$

From system (1), the piezoconductivity equation for the near region (i = 1) can be represented as:

$$\frac{\partial p_{(1)}}{\partial t} = \frac{k_{(1)}}{\phi\left(1 - S_h\right)\rho_s \beta \mu_s} \frac{\partial}{\partial x}\left(\rho_s \frac{\partial p_{(1)}}{\partial x}\right). \tag{5}$$

Similar equations for the intermediate and far regions (i = 2, 3) have the form:

$$\frac{\partial p_{(i)}}{\partial t} = \frac{k_m}{\phi S_m \mu_m} \frac{\partial}{\partial x}\left(p_{(i)} \frac{\partial p_{(i)}}{\partial x}\right). \tag{6}$$

The equation of heat influx after transformations can also be represented as:

$$\frac{\partial T_{(i)}}{\partial t} = \frac{\partial}{\partial x}\left(\kappa^{(T)} \frac{\partial T_{(i)}}{\partial x}\right) + X_{(i)} \frac{\partial p_{(i)}}{\partial x} \frac{\partial T_{(i)}}{\partial x} \ \ (i = 1, 2, 3), \tag{7}$$

where $\kappa^{(T)} = \lambda / \rho C$ is the formation thermal diffusivity; $X_{(1)} = \frac{\kappa^{(T)} \rho_s C_s}{\lambda} \frac{k_{(1)}}{\mu_s}$; $X_{(i)} = \frac{\kappa^{(T)} \rho_m C_m}{\lambda} \frac{k_{(i)}}{\mu_m}$ (i = 2, 3).

To solve a closed system of Equations (5) - (7) with initial boundary conditions (4) and conditions (2) - (3) at the boundaries of the phase transition, the method of catching fronts in the nodes of a spatial grid is used [35].

3. Analysis of the results

In Figure 1 for time t = 10 day. reservoir temperature and pressure distributions are presented. The injection pressure of liquid sulfur dioxide corresponds to the value p_e = 3.2 MPa (fragment *a*) and p_e = 3.1 MPa (fragment *b*). For the remaining parameters characterizing the system, the following values are taken: L = 50 m, ϕ = 0.2, S_{w0} = 0.2, $k_0 = 10^{-15}$ m², G = 0.327, $\mu_s = 3.68 \cdot 10^{-4}$ Pa·s, $\mu_m = 10^{-5}$ Pa·s , λ = 2 W/(m·K), $\rho C = 2 \cdot 10^6$ J/(K·m³), $\beta_s = 1.35 \cdot 10^{-9}$ Pa⁻¹, ρ_h = 1390 kg/m³, ρ_l = 1000 kg/m³, ρ_{w0} = 900 kg/ m³, ρ_{0s} = 1434 kg/m³, C_s = 1350 J/(K·kg), C_m = 1560 J/(K·kg), $L_w = 3.3 \cdot 10^5$ J/kg, $L_h = 2.5 \cdot 10^5$ J/kg, p_0 = 3 MPa, T_e = 268 K, T_0 = 272 K. As follows from Figure 2 and when SO_2 is injected under pressure p_e = 3.2 MPa (fragment *a*), the formation of hydrate occurs according to the formulation presented in the problem with the formation of three regions. When the injection pressure decreases (fragment *b*), the formation of SO_2 hydrate occurs without the formation of a region containing methane and water from sulfur dioxide and ice.

Preprints (www.preprints.org) | NOT PEER-REVIEWED | Posted: 15 June 2023 doi:10.20944/preprints202306.1087.v1

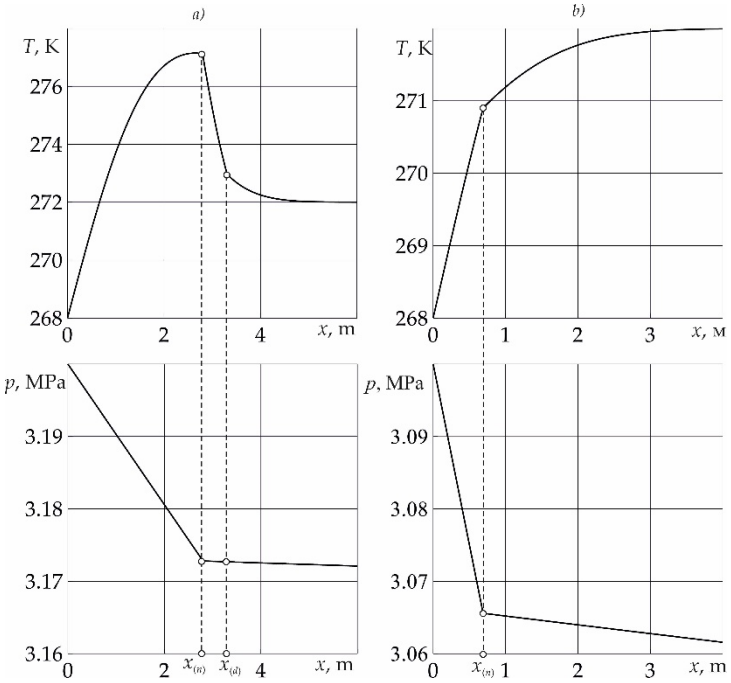

Figure 2. Temperature and pressure distribution in the reservoir for time t = 10 day: *a* – p_e = 3.2 MPa; *b* – p_e = 3.1 MPa.

In Figure 3. for time t = 10 day dependences of the temperature $T_{(n)}$ on the near surface of the phase transition, as well as the coordinates of the near and far boundaries of the phase transition, on the injection pressure p_e are presented. As follows from the figure, with a decrease in the injection pressure, both the temperature at the near boundary of the phase transition and the length of the region containing methane and water decrease. This is due to the fact that with a decrease in the value of p_e, the intensity of the formation of SO_2 hydrate decreases. Thus, in the case of low values of p_e, the intensity of hydrate formation is low and the temperature does not rise above the melting point of ice. In this case, the formation of sulfur dioxide occurs from ice and SO_2 without the formation of a region saturated with methane and water.

Preprints (www.preprints.org) | NOT PEER-REVIEWED | Posted: 15 June 2023 doi:10.20944/preprints202306.1087.v1

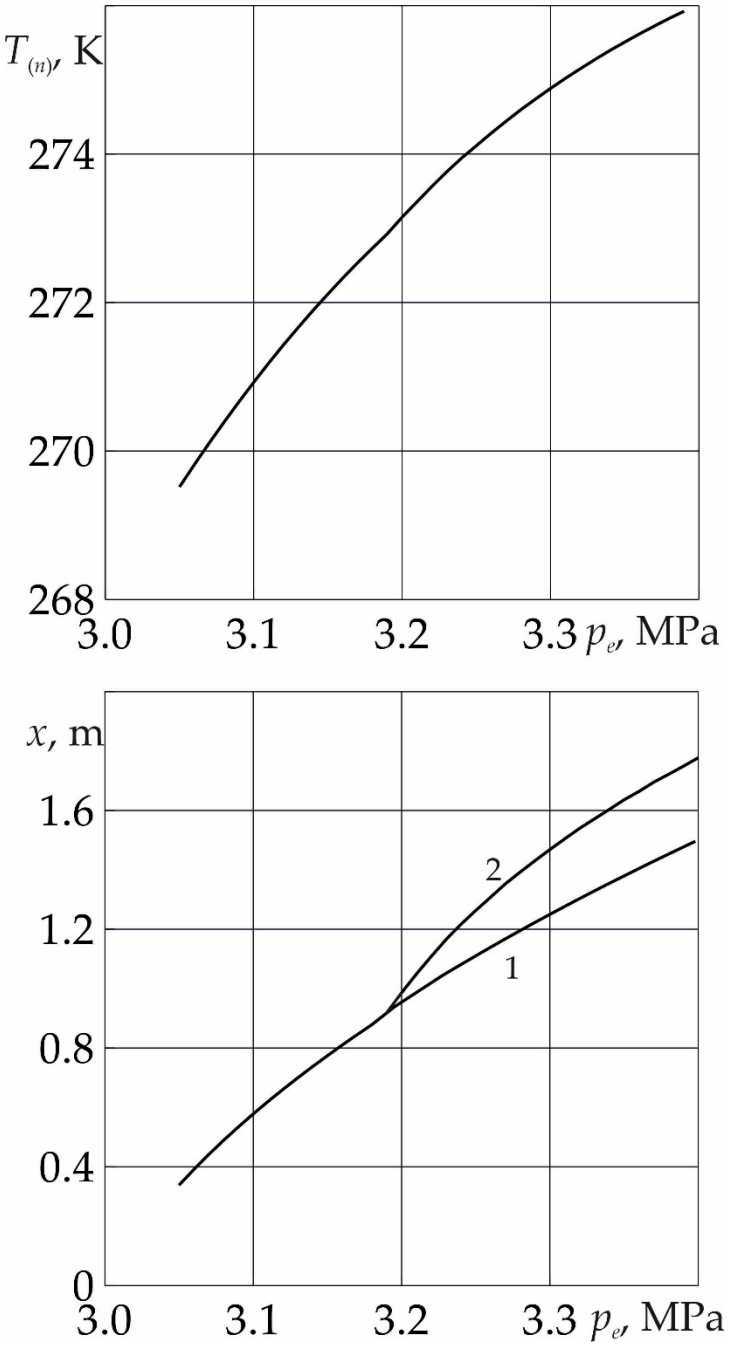

Figure 3. Temperature dependences on the near surface phase transition, as well as the coordinates of the near (1) and far (2) boundaries of the phase transition on the injection pressure.

Figure 4 shows the dependences of the temperature $T_{(n)}$ on the near surface of the phase transition, as well as the coordinates of the near and far boundaries of the phase transition, on the initial pressure of the system. As follows from the figure, with an increase in the initial pressure of the system, both the temperature at the near boundary of the phase transition and the length of the region containing methane and water decrease. This is explained by the fact that as p_0 increases, the pressure drop in the system decreases and, as a consequence of Darcy's law, the intensity of the phase transition decreases. Thus, at high values of p_0, the formation of SO_2 hydrate occurs from ice and sulfur dioxide without the formation of a region saturated with methane and water.

Preprints (www.preprints.org) | NOT PEER-REVIEWED | Posted: 15 June 2023 doi:10.20944/preprints202306.1087.v1

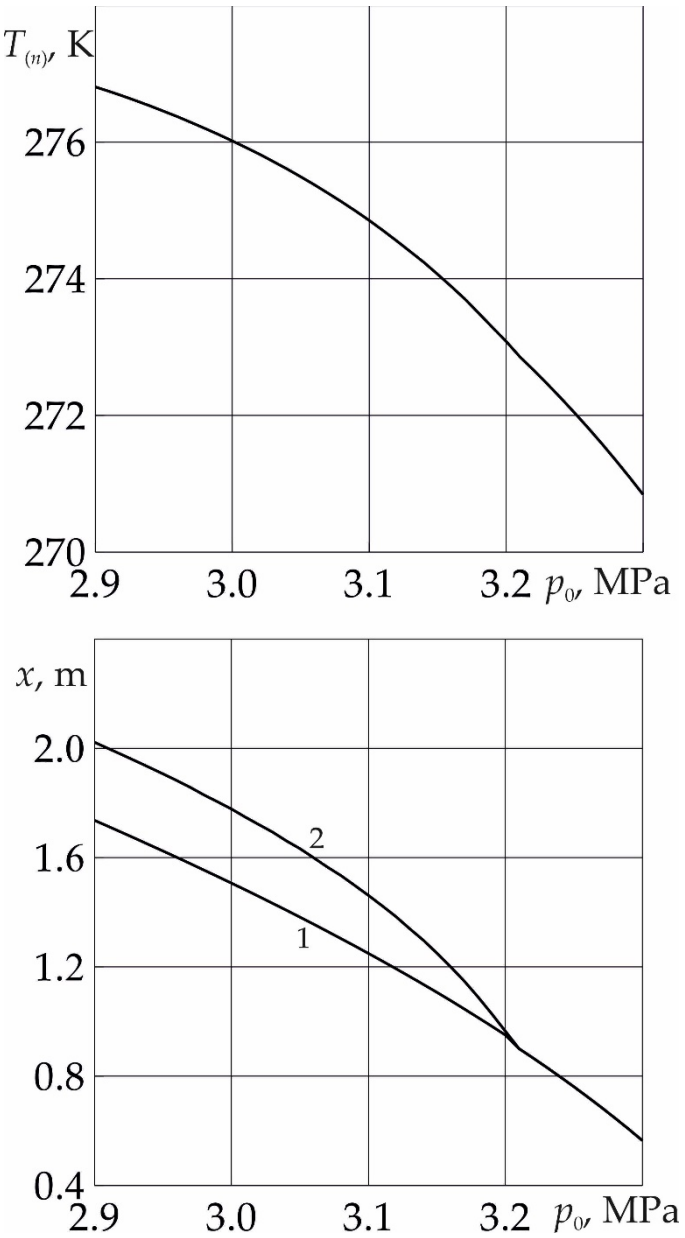

Figure 4. Temperature dependences on the near surface phase transition, as well as the coordinates of the near (1) and far (2) boundaries of the phase transition from the initial pressure of the system.

Figure 5 shows the dependences of the temperature $T_{(n)}$ on the near surface of the phase transition, as well as the coordinates of the near and far boundaries of the phase transition, on the absolute permeability of the reservoir. It follows from the figure that at low values of the absolute permeability of the formation, the formation of sulfur dioxide hydrate occurs from SO_2 and ice. As the value of k_0 increases, the temperature at the phase transition boundary begins to rise. This is due to an increase in the intensity of the phase transition, which is limited by the flow of SO_2 to it and, as follows from the Darcy law, is proportional to the reservoir permeability. In this case, the temperature $T_{(n)}$ can become higher than the melting point of ice. In this case, the formation of SO_2 hydrate occurs with the formation of a region saturated with methane and water.

Preprints (www.preprints.org) | NOT PEER-REVIEWED | Posted: 15 June 2023 doi:10.20944/preprints202306.1087.v1

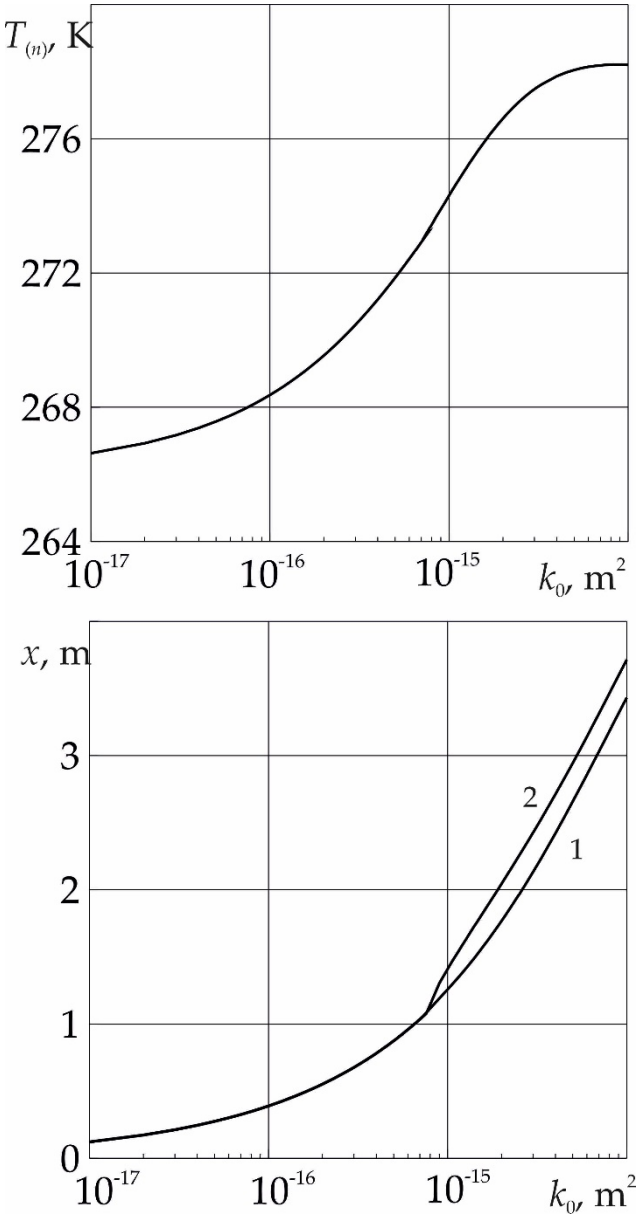

Figure 5. Temperature dependences on the near surface phase transition, as well as the coordinates of the near (1) and far (2) boundaries of the phase transition from the absolute permeability of the reservoir.

Figure 6 shows the dependences of the temperature $T_{(n)}$ on the near surface of the phase transition, as well as the coordinates of the near and far boundaries of the phase transition, on the initial formation temperature (fragment *a*) and injection temperature (fragment *b*) of liquid sulfur dioxide. As follows from the figure, the temperature at the near boundary of the phase transition increases with an increase in both the initial reservoir temperature and the temperature of the injected sulfur dioxide. Thus, as follows from the figure, the formation of sulfur dioxide from SO_2 and water occurs at high initial formation temperature and liquid sulfur dioxide injection temperature.

Preprints (www.preprints.org) | NOT PEER-REVIEWED | Posted: 15 June 2023 doi:10.20944/preprints202306.1087.v1

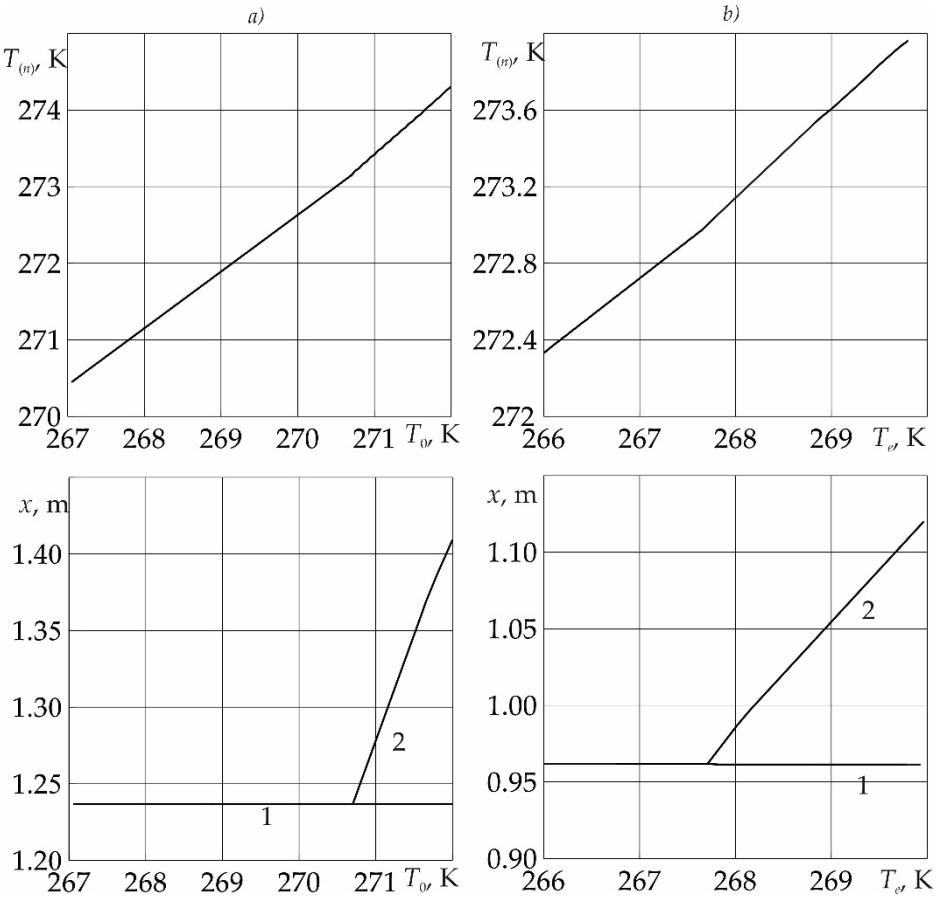

Figure 6. Temperature dependences on the near surface phase transition, as well as the coordinates of the near (1) and far (2) boundaries of the phase transition from the initial reservoir temperature (*a*) and the temperature of the injected sulfur dioxide (*b*).

In Figure 7 for the moment of time t = 10 days the dependence of the critical injection temperature, below which the formation of SO_2 hydrate occurs without the formation of a region saturated with methane and water, on the injection pressure of sulfur dioxide is presented. As follows from the figure, with an increase in the value of p_e, the value of the critical temperature decreases. This is due to the fact that in this case the intensity of the phase transition increases; therefore, the formation of sulfur dioxide hydrate from ice and SO_2 occurs at lower temperatures. In addition, as follows from the figure, the critical temperature also depends on the formation permeability. As the reservoir permeability increases, the critical injection temperature also decreases. This is explained by the fact that an increase in the value of k_0 also leads to an increase in the intensity of the phase transition.

Preprints (www.preprints.org) | NOT PEER-REVIEWED | Posted: 15 June 2023 doi:10.20944/preprints202306.1087.v1

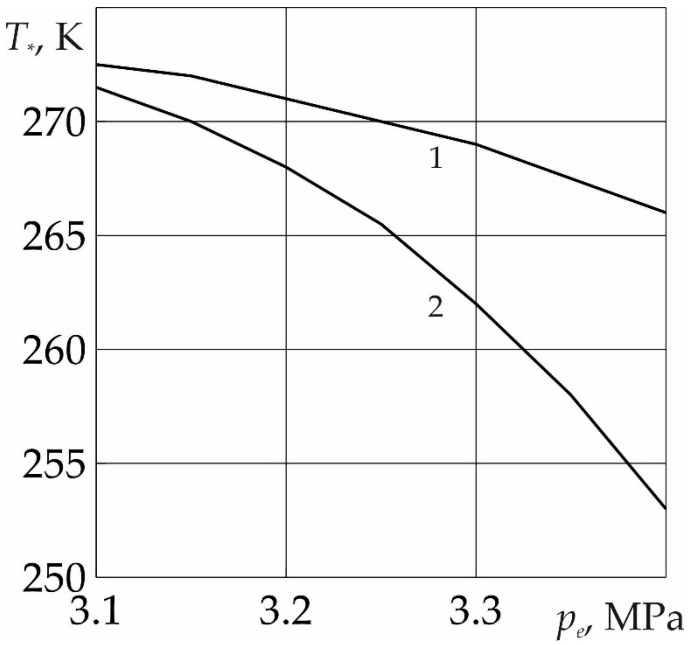

Figure 7. Critical temperature dependences from discharge pressure SO2 at: 1 - $k_0 = 5 \cdot 10^{-16}$ m²; 2 – $k_0 = 10^{-15}$ m².

4. Conclusions

The paper presents a mathematical model of the process of injection of liquid sulfur dioxide into a porous reservoir, initially saturated with methane and ice. The influence of the initial system, as well as the parameters of the injected sulfur dioxide on the features of the formation of SO_2 hydrate in the reservoir, is studied. It has been established that at high values of injection pressure and permeability of the porous reservoir, the formation of SO_2 hydrate occurs with the formation of a region containing methane and water. It is shown that with an increase in the initial pressure of the system, the formation of sulfur dioxide hydrate occurs without the formation of a region saturated with methane and water. It has been established that the formation of sulfur dioxide from SO_2 and water occurs at high values of the initial formation temperature and the injection temperature of liquid sulfur dioxide. The dependence of the critical injection temperature, below which the formation of SO_2 hydrate occurs without the formation of a region saturated with methane and water, on the injection pressure of sulfur dioxide is presented. It is shown that with an increase in the injection pressure, the value of the critical temperature decreases.

Author Contributions: Conceptualization, I.K.G. and M.V.S.; methodology, I.K.G. and M.V.S.; validation, M.V.S.; formal analysis, I.K.G.; investigation, I.K.G. and M.V.S.; writing – original draft preparation, I.K.G. and M.V.S. All authors have read and agreed to the published version of the manuscript.

Data Availability Statement: The data presented in this study are available on request from the corresponding author.

Acknowledgments: State task FEUR - 2023 - 0006, project "Development and creation of low-tonnage products and reagents (corrosion and scale inhibitors, antioxidants, biocides, additives, etc.) for petrochemical processes and water purification from pollution, replacing imported substances and materials. Theoretical and experimental approaches»

Conflicts of Interest: The authors declare no conflict of interest.

References

1. Sloan, E.D., Koh, C.A. *Clathrate Hydrates of Natural Gases*, 3rd ed., Boca Raton: CRC Press, 2007. DOI: 10.1201/9781420008494
2. Carroll, J. *Natural gas Hydrates: a Guide for Engineers*. Gulf Professional Publishing, 2020. DOI: 10.1016/C2013-0-13425-3
3. Makogon, Y.F. Natural gas hydrates - A promising source of energy. J. of Natural Gas Science and Engineering 2010, 2, 49–59. DOI: 10.1016/j.jngse.2009.12.004.
4. Yong, H., Peng, X., Ye Y. Development in technology of prospecting and extraction for gas hydrates. *Geol Prospect* **2002**, 38(1), 70–73
5. Wu, Ch., Zhao, K. Current research in natural gas hydrate production. *Geol Sci Technol Inf.* **2008**, 27(1), 47–52.
6. Ahmadi, G., Ji, C., Smith, D.H. Numerical solution for natural gas production from methane hydrate dissociation. *Journal of Petroleum Science and Engineering* **2004**, 41(4), 269–285.
7. Tsypkin, G.G. Effect of decomposition of a gas hydrate on the gas recovery from a reservoir containing hydrate and gas in the free state. *Fluid Dynamics* **2005**, 40(1), 117-125.
8. Vasil'ev, V.I., Popov, V.V., Tsypkin, G.G. Numerical investigation of the decomposition of gas hydrates coexisting with gas in natural reservoirs. *Fluid Dynamics* **2006**, 41(4), 599-605.
9. Gerami, S., Pooladi-Darvish, M. Predicting gas generation by depressurization of gas hydrates where the sharp-interface assumption is not valid. *J Pet Sci Eng* **2007**, 56(1–3), 146–164.
10. Ahmadi, G., Ji, C., Smith, D.H. Production of natural gas from methane hydrate by a constant downhole pressure well. *Energy Conversion and Management* **2007**, 48(7), 2053–2068. DOI:10.1016/j.enconman.2007.01.015
11. Tsypkin, G.G. Analytical solution of the nonlinear problem of gas hydrate dissociation in a formation. *Fluid Dynamics* **2007**, 42(5), 798-806.
12. Tsypkin, G.G. *Flows with Phase Transitions in Porous Media*, Moscow: Fizmatlit, 2009.
13. Musakaev, N.G., Khasanov, M.K. Solution of the Problem of Natural Gas Storages Creating in Gas Hydrate State in Porous Reservoirs. *Mathematics* **2020**, 8(1), 36. DOI: 10.3390/math8010036
14. Musakaev, N.G., Borodin, S.L., Gubaidullin, A.A. Methodology for the Numerical Study of the Methane Hydrate Formation During Gas Injection into a Porous Medium. *Lobachevskii Journal of Mathematics* **2020**, 41(7), 1272–1277. DOI: 10.1134/S199508022007032X
15. Borodin, S.L., Musakaev, N.G., Belskikh, D.S. Mathematical Modeling of a Non-Isothermal Flow in a Porous Medium Considering Gas Hydrate Decomposition: A Review. *Mathematics* **2022**, 10(24), 4674. DOI: 10.3390/math10244674
16. Shitz, E.Yu., Koryakina, V.V., Ivanova, I.K., Semenov M.E. Research on growth kinetics and growth mechanism of natural gas hydrates in water-in-asphaltene-resin-paraffin deposits (ARPD) and water-in-oil emulsions. *Chemistry for Sustainable Development* **2018**, 26(3), 271-280.
17. Ivantsova, A.O., Lyubimova, T.P., Lyubimov, D.V. Dynamics of vertical channel penetrating hydrate layer. *Bulletin of Perm university. Series: Physics* **2012**, 4(22), 65-68.
18. Misyura, S.Y., Donskoy, I.G. Dissociation and combustion of a layer of methane hydrate powder: ways to increase the efficiency of combustion and degassing. *Energies* **2021**, 14(16), 4855. DOI: 10.3390/en14164855
19. Zhao, J., Xu, K., Song, Y., Liu, W., Lam, W., Liu, Y., Xue, K., Zhu, Y., Yu, X., Li, Q. A Review on Research on Replacement of CH_4 in Natural Gas Hydrates by Use of CO_2. *Energies* **2012**, 5, 1-21. DOI:10.3390/EN5020399
20. Voronov, V.P., Gorodetskii, E.E, Muratov, A.R. Experimental study of methane replacement in gas hydrate by carbon dioxide. *J Phys Chem B.* **2010**, 114(38), 12314-12318. DOI: 10.1021/jp104821p
21. Nago, A., Nieto, A. Natural gas production from methane hydrate deposits using CO2 clathrate sequestration: Stateof-the-art review and new technical approaches *J. Geol. Res.* **2011**, 239397, 1–6. DOI:10.1155/2011/239397
22. Parshall, J. Production Method for Methane Hydrate Sees Scientific Success. *J. of Petroleum Technology* **2012**, 64, 50–51. DOI:10.2118/0812-0050-JPT
23. Kvamme, B., Graue, A., Buanes, T., Kuznetsova, T., Ersland, G. Storage of CO_2 in natural gas hydrate reservoirs and the effect of hydrate as an extra sealing in cold aquifers. *International Journal of Greenhouse Gas Control* **2007**, 1, 236-246. DOI:10.1016/S1750-5836(06)00002-8
24. White, M.D., McGrail, P.B.. Designing a pilot-scale experiment for the production of natural gas hydrates and sequestration of CO2 in class 1 hydrate accumulations. *Energy Procedia* **2009**, 1, 3099-3106. DOI:10.1016/J.EGYPRO.2009.02.090
25. Garapati, N., Velaga, S.C., Anderson, B.J. Development of a thermodynamic framework for the simulation of mixed gas hydrates: formation, dissociation, and CO_2-CH_4 exchange. *Proceedings of the 7 International Conference on Gas Hydrates. Edinburg, UK* 2011.
26. Lackner, K.S. A Guide to CO_2 Sequestration. *Science* **2003**, 300, 1677–1678. DOI:10.1126/SCIENCE.1079033

27. Kang, Q., Lichtner, P., Viswanathan, H.S., Abdel-Fattah, A.I. Pore Scale Modeling of Reactive Transport Involved in Geologic CO_2 Sequestration. *Transport in Porous Media* **2010**, 82, 197-213. DOI:10.1007/S11242-009-9443-9
28. Benson, S.M., Cole, D.R. CO_2 Sequestration in Deep Sedimentary Formations. *Elements* **2008**, 4, 325-331. DOI:10.2113/GSELEMENTS.4.5.325
29. Anshits, A., Kirik, N., Shibistov, B. Possibilities of SO_2 storage in geological strata of permafrost terrain. *Advances in the Geological Storage of Carbon Dioxide* **2006,** 65, 93-102. DOI:10.1007/1-4020-4471-2_09
30. Li, Q., Li, X., Wei, N., Fang, Z. Possibilities and potentials of geological co-storage CO2 and SO2 in China. *Energy Procedia* **2011**, 4, 6015-6020. DOI:10.1016/J.EGYPRO.2011.02.605
31. Istomin, V.A., Yakushev, V.S. *Gas hydrates in nature*. Nedra: Moscow, Russia, 1992.
32. Khasanov, M.K., Stolpovsky, M.V., Gimaltdinov, I.K. Mathematical model for carbon dioxide injection into porous medium saturated with methane and gas hydrate. *International Journal of Heat and Mass Transfer* **2018**, 127, 21 – 28.
33. Khasanov, M.K., Stolpovsky, M.V., Gimaltdinov, I.K. Mathematical model of injection of liquid carbon dioxide in a reservoir saturated with methane and its hydrate. *International Journal of Heat and Mass Transfer* **2019**, 132, 529 – 538.
34. Barenblatt, G.I., Entov, V.M., Ryzhik, V.M. Movement of liquids and gases in natural formations. Nedra: Moscow, Russia, 1982.
35. Samarskij, A.A., Vabishchevich, P.N. Computational heat transfer. Editorial URSS: Moscow, Russia, 2003.